Observational Study

Medicine®

OPEN

Triphasic dynamic contrast-enhanced computed tomography predictive model of benign and malignant risk of gallbladder occupying lesions

Jinqiu Tao, MD[a], Yanqiu Zhang, MM[b], Huihui Chen, MM[a], Shaohe Wang, MM[a], Qi Sun, MD[c], Wenjie Zhang, PhD[a], Qiaoyu Liu, MD[a], Xiaoli Mai, PhD[b,*], Decai Yu, PhD[a,*]

Abstract

Gallbladder occupying lesions are common diseases of biliary system. Among them, gallbladder cancer is difficult to diagnose due to the indistinguishable early symptoms, thus posing a great risk to the population. This study aims to establish a computed tomography (CT) prediction model for distinguishing benign and malignant lesions of gallbladder occupying lesions.

The study included 211 patients with benign or malignant gallbladder occupying lesions who have taken resection in the Nanjing Drum Tower Hospital from January 2009 to December 2017. Clinical data collected includes age and sex; CT data includes tumor location, tumor maximum diameter, tumor form, venous phase portal venous CT value, abdominal aortic CT value, plain phase CT value, arterial phase CT value, venous phase CT value, delayed phase CT value, ΔCT_1, ΔCT_2, ΔCT_3, ΔCT_4, ΔCT_5, ΔCT_6, and ΔCT_7. Calculation of odds ratio between benign and malignant gallbladder occupying lesions using single factor screening variables and multivariate logistic regression was done to establish a model and calculate the areas under receiver operating characteristic curves of the model.

Multivariate logistic regression analysis showed that age, tumor maximum diameter, tumor form, venous phase portal venous CT value, ΔCT_2, ΔCT_4, and ΔCT_6 are the main characteristic index for differential diagnosis of benign and malignant risk of gallbladder occupying lesions.

Patients' age, tumor maximum diameter, tumor form, venous phase portal venous CT value, ΔCT_2, ΔCT_4, and ΔCT_6 are independent risk factors for judging the benign and malignant of gallbladder occupying lesions. The model established exhibited a potential diagnostic value for distinguishing the malignant properties of gallbladder occupying lesions.

Abbreviations: AUC = area under curve, CT = computed tomography, ΔCT_1 = arterial phase CT value minus plain phase CT value, ΔCT_2 = venous phase CT value minus plain phase CT value, ΔCT_3 = delayed phase CT value minus arterial phase CT value, ΔCT_4 = venous phase portal venous CT value minus delayed phase CT value, ΔCT_5 = plain phase CT value minus arterial phase CT value, ΔCT_6 = plain phase CT value minus delayed phase CT value, ΔCT_7 = venous phase CT value minus venous phase portal venous CT value, OR = odds ratio, ROC = receiver operating characteristic.

Keywords: computed tomography, diagnosis, gallbladder cancer, logistic models

1. Introduction

Gallbladder occupying lesions mainly include gallbladder polyps, cholecystitis, gallbladder adenomyosis, gallbladder cancer, etc; among them, gallbladder cancer has a high mortality rate, a poor prognosis, and ranks fourth in the incidence of malignant gastrointestinal cancer in China.[1,2] Besides, the early symptoms of gallbladder cancer are unspecific, and patients with liver metastases are often diagnosed at the initial diagnosis.[3,4] Studies have shown that early surgery for gallbladder cancer would achieve a 5-year survival rate more than 80%.[5–7] However, early gallbladder cancer has no obvious clinical signs and symptoms. Most patients have been in advanced stage at the time of treatment, while local or distant metastasis significantly reduced the chance of surgical resection. The prognosis of patients with advanced gallbladder cancer is poor with a survival rate of only 13%.[8] Therefore, early identification and diagnosis of benign and malignant gallbladder occupying lesions is of great importance to improve the prognosis of patients.

Nowadays, abdominal ultrasound is still the first-line examination method for patients with gallbladder occupying lesions. With the development of science and technology, a large number of advanced diagnostic methods have been appearing,

Editor: Goran Augustin.

JT, YZ, HC, and SW contributed equally to this work.

The datasets generated during and/or analyzed during the current study are available from the corresponding author on reasonable request.

This work was supported by the Key Project supported by Medical Science and Technology Development Foundation, Nanjing Department of Health (YKK16108, ZKX17016).

The authors have no conflicts of interest to disclose.

[a] Department of General Surgery, [b] Department of Radiology, [c] Department of Pathology, the Affiliated Drum Tower Hospital of Medical School of Nanjing University, Nanjing, China.

[*] Correspondence: Decai Yu, Nanjing Drum Tower Hospital Department of Liver and Gall Bladder Surgery, Nanjing, China (e-mail: yudecai2019@sina.com); Xiaoli Mai, Department of Radiology, the Affiliated Drum Tower Hospital of Medical School of Nanjing University, Nanjing, China (e-mail: MaiXL@njglyy.com).

How to cite this article: Tao J, Zhang Y, Chen H, Wang S, Sun Q, Zhang W, Liu Q, Mai X, Yu D. Triphasic dynamic contrast-enhanced computed tomography predictive model of benign and malignant risk of gallbladder occupying lesions. Medicine 2020;99:13(e19539).

Received: 22 November 2019 / Received in final form: 12 February 2020 / Accepted: 13 February 2020

http://dx.doi.org/10.1097/MD.0000000000019539

such as the contrast-enhanced ultrasound, endoscopic ultrasound, computed tomography (CT), magnetic resonance imaging, and positron emission tomography/CT.[9] However, these modern imaging techniques cannot reliably identify the benign and malignant properties of tumors.[2,10,11] Ultrasound is the first choice for the diagnosis of gallbladder disease with the correct rate of diagnosis at 70% to 82%, while the detection rate for gallbladder cancer is only 23%.[12] It is difficult for the traditional CT examination to identify gallbladder occupying lesions less than 10 mm.[13] And now, the application of multi-slice spiral CT has remarkably improved the accuracy of CT in the diagnosis of gallbladder occupying lesions. What is more, CT-enhanced scan can show the morphology, hemodynamic changes, surrounding tissue structure, and tumor metastasis of gallbladder carcinoma, so as to evaluate the lesion stage.[14] Recently, some scholars have reported that triphasic dynamic contrast-enhanced CT can predict the benign and malignant risk of gallbladder occupying lesions.[2] However, previous studies evaluated the benign and malignant of gallbladder occupying lesions via a single-factor model, and the effects of other factors on the model were not considered. Therefore, a more objective and simple method for predicting gallbladder occupying lesions is urgently needed. The purpose of this study was to establish a simple and accurate risk model that can predict the benign and malignant of gallbladder occupying lesions by preoperative CT examination and thus provide assistance for subsequent surgery.

2. Materials and methods

2.1. General information

This study retrospectively analyzed 211 cases of patients with gallbladder occupying lesions who underwent general surgical resection and clear pathological diagnosis in the Nanjing Drum Tower Hospital from January 2009 to December 2017. The consent was obtained from the Ethics Committee of Nanjing Drum Tower Hospital. According to the pathological results of cholecystectomy, all the subjects were divided into the malignant of gallbladder occupying lesions and the benign of gallbladder occupying lesions.

2.2. Imaging techniques and analysis

All patients underwent a supine position multi-slice helical CT (Lightspeed, VCT, or Discovery HD750, GE Healthcare, Milwaukee, WI) non-contrast scan and enhanced scan. The scan range was from the septum to the pubic union level. Scanning parameters were as follows: slice thickness, 5 mm; slice interval, 5 mm; reconstructed slice thickness, 1.25 mm; tube voltage, 120 kVp; tube current, 240 mA; helical pitch, 1.375. After CT non-contrast scan, 3-phase dynamic contrast scan was performed. Non-ionic contrast agent (Omnipaque 350 mg I/mL, GE Healthcare, Milwaukee, WI) was injected into elbow vein with high-pressure syringe (MedradStellant, Indianola, PA) at an injection rate of 3.0 Indianola mL/S and an injection dose of 80 mL, followed by 20 mL saline at the same rate. After injection, the arterial phase was achieved with a delay time of 30 seconds and portal venous phase with 70 seconds, delayed phase with 3 minutes. Two senior experienced radiologists and 1 senior general surgeon who did not inform the pathologic results interpreted the CT images independently. If there was inconsistency, consensus was achieved through discussion with a third chief radiologist. All the examination items were as follows: the location of the lesion, the maximum diameter of the lesion (for patients with more than 1 lesion, the largest lesion was measured, and the maximum diameter of the lesion was between 0.5 and 6.0 cm.), and the shape of the lesion. Quantitative analysis was also performed. The region of interest was placed in the solid part of the lesion that showed the most remarkable enhancement and avoided the area of necrosis. The measurement parameters included: arterial phase CT value (measured value minus simultaneous abdominal arterial phase CT value), venous phase CT value (measured value minus simultaneous abdominal arterial phase CT value), delayed phase CT value (measured value minus simultaneous abdominal arterial phase CT value), venous phase portal venous CT value, ΔCT_1 (arterial phase CT value minus plain phase CT value), ΔCT_2 (venous phase CT value minus plain phase CT value), ΔCT_3 (delayed phase CT value minus arterial phase CT value), ΔCT_4 (venous phase portal venous CT value minus delayed phase CT value), ΔCT_5 (plain phase CT value minus arterial phase CT value), ΔCT_6 (plain phase CT value minus delayed phase CT value), and ΔCT_7 (venous phase CT value minus venous phase portal venous CT value). Three regions of interest were selected by each observer, and the average value was taken. The average value calculated by the 2 radiologists and 1 senior general surgeon is the final result. The typical CT image of benign and malignant lesions is shown below.

2.3. Statistical analysis

Statistical analysis was performed using R-3.6.0, the count data were described by percentage, and the measurement data were presented as mean ± standard deviation. The difference was statistically significant at $P < .05$. Univariate logistic regression analysis was used for all variables, and the results of univariate analysis ($P < .2$) were included in multivariate logistic regression analysis. The model with the smallest AIC (Akaike information criterion) index was selected by backward stepwise regression method to screen for pathological benign and malignant related independent risk factors.

3. Results

3.1. General information and baseline characteristics

Among the 211 cases included in the study, 98 cases (46.4%) were confirmed by postoperative pathology as malignant of gallbladder occupying lesions, and 113 cases (53.6%) were confirmed as benign of gallbladder occupying lesions. The complete clinical and CT data of these patients included 119 females and 92 males aged from 22 to 90 (58 ± 11.91, mean ± SD) years. Among the patients with malignant of gallbladder occupying lesions, 39 (18.48%) were male and 59 (27.96%) were female. The mean age was 55.57 ± 12.41 years for patients with benign gallbladder occupying lesions and 61.77 ± 10.40 (mean ± SD) years for the patients with malignant gallbladder occupying lesions with a significant difference ($P < .001$). However, no significant difference of sex was observed between the 2 groups (Table 1).

3.2. Imaging features of the benign and malignant of gallbladder occupying lesions

Abdominal CT image of a benign gallbladder lesion of a 49-year-old woman was shown (Figure 1A). The lesion is located in the body of the gallbladder; the maximum lesion diameter was 1.5

Table 1

Baseline characteristics and univariate logistic regression analysis of total points in the malignant of gallbladder occupying lesions.

Characteristic	Benign (n = 113)	Malignant (n = 98)	*P* value
Age, yr, mean ± SD	55.57 ± 12.41	61.77 ± 10.40	<.001*
Sex, n (%)			.29
Male	53 (25.12%)	39 (18.48%)	
Female	60 (28.44%)	59 (27.96%)	
Tumor maximum diameter, cm, mean ± SD	1.3 ± 0.76	2.35 ± 1.21	<.001*
Tumor form, n (%)			.061
Mass type	86 (40.76%)	63 (29.86%)	
Non-mass type	27 (12.80%)	35 (16.58%)	
Plain phase CT value, HU, mean ± SD	−14.08 ± 10.42	−4.5 ± 8.88	<.001*
Arterial phase CT value, HU, mean ± SD	55.50 ± 20.67	66.19 ± 21.00	<.001*
Venous phase CT value, HU, mean ± SD	−71.91 ± 22.20	−73.74 ± 27.88	.59
Venous phase portal venous CT value, HU, mean ± SD	158.33 ± 40.42	168.39 ± 42.45	.081
Delayed phase CT value, HU, mean ± SD	−42.41 ± 22.78	−34.96 ± 18.51	.012*
ΔCT_1, HU, mean ± SD	−227.86 ± 77.75	−246.99 ± 69.90	.064
ΔCT_2, HU, mean ± SD	−57.82 ± 22.53	−69.24 ± 30.82	.0034*
ΔCT_3, HU, mean ± SD	199.54 ± 73.14	216.52 ± 62.87	.076
ΔCT_4, HU, mean ± SD	87.06 ± 27.16	83.85 ± 29.86	.4
ΔCT_5, HU, mean ± SD	−25.90 ± 17.66	−27.97 ± 20.69	.432
ΔCT_6, HU, mean ± SD	−41.66 ± 22.85	−46.31 ± 23.14	.14
ΔCT_7, HU, mean ± SD	4.69 ± 13.95	1.04 ± 14.02	.062

CT, computed tomography, ΔCT_1 = arterial phase CT value minus plain phase CT value, ΔCT_2 = venous phase CT value minus plain phase CT value, ΔCT_3 = delayed phase CT value minus arterial phase CT value, ΔCT_4 = venous phase portal venous CT value minus delayed phase CT value, ΔCT_5 = plain phase CT value minus arterial phase CT value, ΔCT_6 = plain phase CT value minus delayed phase CT value, ΔCT_7 = venous phase CT value minus venous phase portal venous CT value, SD = standard deviation.

cm. Postoperative pathologic slices showed tubular adenoma with low grade dysplasia. Abdominal CT image of a malignant gallbladder lesion of a 46-year-old woman was also displayed (Figure 1B). The lesion is located in the bottom of the gallbladder, and the maximum lesion diameter was 2.9 cm. Postoperative pathologic slices showed papillary adenocarcinoma.

3.3. Univariate correlation analysis and multivariate logistic regression analysis

The single factor analysis of imaging parameters showed that the maximum diameter of the tumor in the malignant group was significantly higher than that in the benign group ($P < .001$). The plain phase CT value, the arterial phase CT value, the delayed

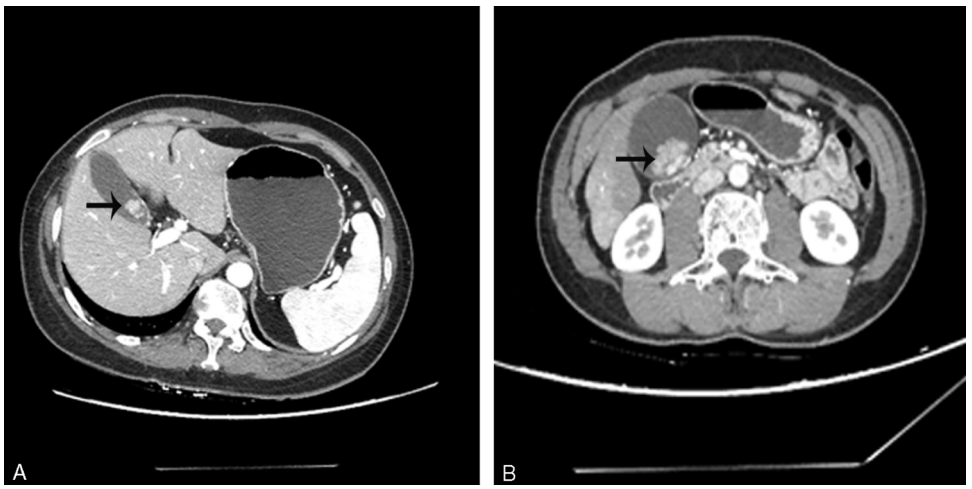

Figure 1. Comparison of CT images between benign and malignant of gallbladder occupying lesions. (A) The lesion is located in the body of the gallbladder and the maximum lesion diameter was 1.5 cm. Postoperative pathologic slices showed tubular adenoma with low grade dysplasia. The CT values of the lesions in plain scan, arterial phase, venous phase, and delayed phase were -12HU, -323HU, -81HU, and -81HU, respectively. Portal vein CT value in venous phase was 277HU, ΔCT_1 was -311HU, ΔCT_2 was -69HU, ΔCT_3 was 242HU, ΔCT_4 was 358HU, ΔCT_5 was 311HU, ΔCT_6 was 69HU, and ΔCT_7 was 358HU. (B) The lesion is located in the bottom of the gallbladder, and the maximum lesion diameter was 2.9 cm. Postoperative pathologic slices showed papillary adenocarcinoma. The CT values of the lesions in plain scan, arterial phase, venous phase, and delayed phase were -4HU, -252HU, -64HU, and -43HU, respectively. Portal venous CT value in venous phase was 168HU, ΔCT_1 was -248HU, ΔCT_2 was 188HU, ΔCT_3 was 209HU, ΔCT_4 was 211HU, ΔCT_5 was 248HU, ΔCT_6 was 39HU, and ΔCT_7 was 232HU. CT = computed tomography, ΔCT_1 = arterial phase CT value minus plain phase CT value, ΔCT_2 = venous phase CT value minus plain phase CT value, ΔCT_3 = delayed phase CT value minus arterial phase CT value, ΔCT_4 = venous phase portal venous CT value minus delayed phase CT value, ΔCT_5 = plain phase CT value minus arterial phase CT value, ΔCT_6 = plain phase CT value minus delayed phase CT value, ΔCT_7 = venous phase CT value minus venous phase portal venous CT value.

phase CT value, and the ΔCT_2 value between the 2 groups were significantly different ($P < .05$). No marked difference of the tumor form, venous phase CT value, venous phase portal venous CT value, ΔCT_1, ΔCT_3, ΔCT_4, ΔCT_5, and ΔCT_6 was observed between the 2 groups ($P > .05$) (Table 1). Subsequently, we included age, sex, tumor maximum diameter, tumor form, venous phase portal venous CT value, ΔCT_1, ΔCT_2, ΔCT_3, ΔCT_4, ΔCT_5, and ΔCT_6 into a multivariate logistic regression analysis. The results were as follows: age (odds ratio [OR] = 1.049), sex (OR = 0.784), tumor maximum diameter (OR = 4.151), tumor form (OR = 0.149), venous phase portal venous CT value (OR = 1.057), ΔCT_1 (OR = 0.997), ΔCT_2 (OR = 0.974), ΔCT_3 (OR = 0.998), ΔCT_4 (OR = 0.925), ΔCT_5 (OR = 0.978), and ΔCT_6 (OR = 1.061). Age, tumor maximum diameter, tumor form, venous phase portal venous CT value, ΔCT_2, ΔCT_4, and ΔCT_6 of the above results were independent risk factors for predicting the malignant of gallbladder occupying lesions ($P < .05$) (Table 2).

3.4. Logistic regression multivariate analysis diagnostic model boundary value and area under receiver operating characteristic (ROC curve)

Diagnostic model was established by several independent risk factors including age, maximum tumor, tumor form, venous phase portal vein CT value, ΔCT_2, ΔCT_4, and ΔCT_6. Logistic regression equation: $\ln\left(\frac{P}{1-P}\right) = -6.61 + 0.047 \times \text{Age} - 0.24 \times \text{Sex} + 1.42 \times \text{Tumor maximum diameter} - 1.9 \times \text{Tumor form} - 0.0029 \times \Delta CT_1 - 0.0025 \times \Delta CT_2 + 0.055 \times \text{Venous phase portal venous CT value} - 0.0017 \times \Delta CT_3 - 0.077 \times \Delta CT_4 - 0.022 \times \Delta CT_5 + 0.059 \times \Delta CT_6$. The ROC curve was drawn according to the above logistic regression equation. The area under curve (AUC) was 0.875, the accuracy of the logistic regression model for the benign and malignant of gallbladder occupying lesions was 80.5% (170/211), the sensitivity was 86.7% (85/98), the specificity was 75.2% (85/113), the positive predictive value was 75.2% (85/113), the negative predictive value was 86.7% (85/98), and the predicted cutoff value was 0.428 (Figure 2).

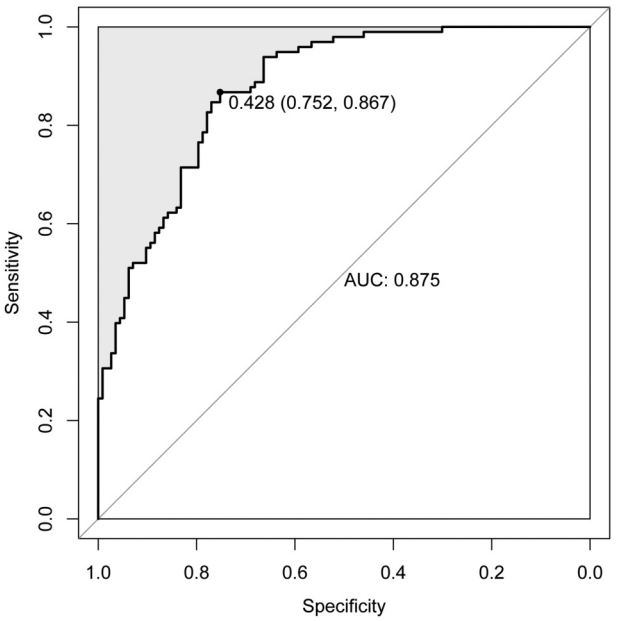

Figure 2. ROC curve of multivariate logistic analysis model in predicting the malignant lesion of the gallbladder occupying lesion shows the AUC of 0.875. AUC = area under curve, ROC = receiver operating characteristic curve.

3.5. Construction of a nomogram model

Including all the independent risk factors related to benign and malignant lesions of gallbladder occupying lesions obtained from above the multivariate analysis, we used R-software to establish a predictive nomogram model (Figure 3). In practice, the clinician can add scores corresponding to various risk factors to obtain a total score, and thereby know the probability of a malignant lesion of the gallbladder occupying lesion to determine the next treatment. The value on each scale of the forecast indicator corresponds to the score of the points. The scores of all the indicators are added to obtain the total score and the total score corresponds to the risk prediction value.

4. Discussion

At present, surgical treatment is still the only way to cure gallbladder cancer. Although adjuvant chemotherapy has been paid more and more attention in recent years, the curative effect is still inaccurate. Because the clinical symptoms of gallbladder cancer are not typical, the patients are often accompanied by

Table 2

Multivariate logistic regression analysis of possible variables in predicting the malignant of gallbladder occupying lesions.

Characteristic	Beta	*P* value	OR (95% CI)
Age	0.047	<.001*	1.049 (0.012, 0.085)
Sex	−0.24	.59	0.784 (−1.14, 0.652)
Tumor maximum diameter (cm)	1.42	<.001*	4.151 (0.931, 1.993)
Tumor form	−1.9	<.001*	0.149 (−2.927, −0.959)
Venous phase portal venous CT value	0.055	.011*	1.057 (0.013, 0.099)
ΔCT_1	−0.0029	.84	0.997 (−0.032, 0.026)
ΔCT_2	−0.025	.046*	0.974 (−0.05, -0.0009)
ΔCT_3	−0.0017	.91	0.998 (−0.031, 0.028)
ΔCT_4	−0.077	<.001*	0.925 (−0.124, -0.033)
ΔCT_5	−0.022	.07	0.978 (−0.046, 0.001)
ΔCT_6	0.059	.010*	1.061 (0.014, 0.106)

CT, computed tomography, ΔCT_1 = arterial phase CT value minus plain phase CT value, ΔCT_2 = venous phase CT value minus plain phase CT value, ΔCT_3 = delayed phase CT value minus arterial phase CT value, ΔCT_4 = venous phase portal venous CT value minus delayed phase CT value, ΔCT_5 = plain phase CT value minus arterial phase CT value, ΔCT_6 = plain phase CT value minus delayed phase CT value, ΔCT_7 = venous phase CT value minus venous phase portal venous CT value, OR = odds ratio.

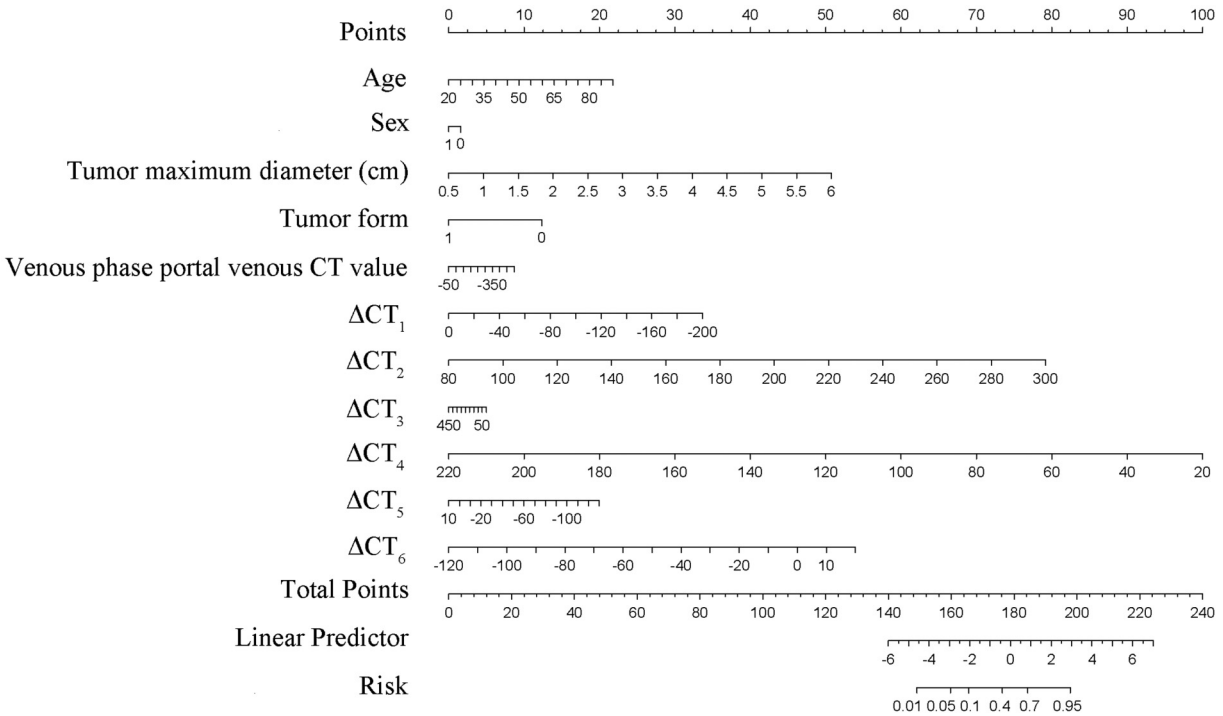

Figure 3. Predictive nomogram for the probability of gallbladder cancer in the gallbladder occupying lesion of patients.

lymph node metastasis and distant metastasis. Data have shown that only 10% of patients meet the indication for surgical resection at the time of diagnosis.[15,16] Due to the insidious onset of gallbladder cancer, the diagnostic accuracy of early gallbladder cancer was only 23%, which is mainly attributed to the non-specific tumor markers, imaging examinations, and other methods widely used in the clinical diagnosis difference between the early malignant and benign of the gallbladder. Recently, the incidence of gallbladder cancer has significantly increased in younger population and is more common in women. Studies have indicated that gallstones and chronic cholecystitis are important risk factors for gallbladder cancer, and more than 85% of patients with gallbladder cancer have gallstones.[17,18] Nowadays, with the advancement of technology, tumor markers, imaging examinations, and other methods are widely used in clinical diagnosis; however, these were still not enough to accurately confirm the nature of gallbladder occupying lesions before surgery.[9,19] Clinically, triphasic dynamic contrast-enhanced CT scans are often used to examine the vital organs of the abdomen, such as the liver, gallbladder, pancreas, and spleen. Previous studies have attempted to predict the benign and malignant gallbladder occupying lesions by preoperative use of clinical data and triphasic dynamic contrast-enhanced CT scans data.[2,20]

Studies have reported single-factor model to assess the benign and malignant of gallbladder occupying lesions.[2] However, these studies are 1-sided and limited because they often do not consider the influence of other factors on the model. Our research model has obvious advantages over previous research. First, there are many specific signs of gallbladder occupying lesions, and the multi-factor analysis model can make up for the defects of single factor diagnosis. Secondly, the simple and objective quantitative scoring method of this system is convenient for clinical application, and the imaging doctors can score the specific signs according to the objective scores to judge the malignant risk of gallbladder occupying lesions rather than just providing descriptive conclusions of the model. Specifically, we first used single factor logistic regression to screen out the variables with *P*-value less than .2 and included them in multi-factor logistic analysis. Then, the backward stepwise regression was used to establish a research model to calculate the OR value of each variable. We have come to a conclusion that the age (OR = 1.049), tumor maximum diameter (OR = 4.151), tumor form (OR = 0.149), venous phase portal venous CT value (OR = 1.057), ΔCT_2 (OR = 0.974), ΔCT_4 (OR = 0.925), and ΔCT_6 (OR = 1.061) were the main characteristic index for differential diagnosis of benign and malignant risk of gallbladder occupying lesions. It is indicated that the 11 characteristic indexes mentioned above have more important significance in distinguishing the benign and malignant gallbladder occupying lesions. Besides, according to the OR value of these indicators, the weight of the gallbladder occupying lesions should be emphasized in clinical diagnosis. Combined with clinical and other imaging features, our model will have a higher accuracy in determining the benign and malignant of the benign and malignant gallbladder occupying lesions.

The ROC curve is a comprehensive indicator of continuous variables of the sensitivity and specificity, and the area under the ROC curve quantitatively indicates the accuracy of the diagnosis. The AUC of this prediction model is as high as 0.875, and the sensitivity, specificity, and the prediction accuracy are 86.7%, 75.2%, and 80.5% respectively. The cutoff value is 0.428, which means the diagnosis may be considered malignant if the risk probability of predicting malignancy is greater than 42.8%. Our results showed that the curve has a satisfactory goodness of fit and predictive effect, and has a high application value in the differential diagnosis of benign and malignant lesions of gallbladder space.

There are also some limitations in this study. The study is a single-center study. Because of the information bias and selection bias in retrospective studies, the multi-center integration research is warranted in future studies. In addition, prospective double-blind case-control studies and increased sample size are also going to be adapted to reduce bias in subsequent studies.

5. Conclusion

The present study demonstrated that the patient's age, maximum tumor, tumor form, venous phase portal venous CT value, ΔCT_2, ΔCT_4, and ΔCT_6 were independent risk factors for judging the benign and malignant of gallbladder occupying lesions. The model established in this study has a good diagnostic effect, which could help clinicians to distinguish the benign and malignant properties of gallbladder occupying lesions and provide assistance for subsequent surgical treatment.

Author contributions

Conceptualization: Decai Yu, Xiaoli Mai.
Data curation: Jinqiu Tao, Yanqiu Zhang, Shaohe Wang, Huihui Chen.
Formal analysis: Wenjie Zhang, Qiaoyu Liu.
Funding acquisition: Jinqiu Tao, Xiaoli Mai.
Investigation: Huihui Chen.
Methodology: Huihui Chen, Jinqiu Tao.
Resources: Qi Sun.
Software: Huihui Chen.
Writing – original draft: Jinqiu Tao.
Writing – review & editing: Deicai Yu, Xiaoli Mai.

References

[1] Bray F, Ferlay J, Soerjomataram I, et al. Global cancer statistics 2018: GLOBOCAN estimates of incidence and mortality worldwide for 36 cancers in 185 countries. CA Cancer J Clin 2018;68:394–424.
[2] Zhou W, Li G, Ren L. Triphasic dynamic contrast-enhanced computed tomography in the differentiation of benign and malignant gallbladder polypoid lesions. J Am Coll Surg 2017;225:243–8.
[3] Wernberg JA, Lucarelli DD. Gallbladder cancer. Surg Clin North Am 2014;94:343–60.
[4] Gourgiotis S, Kocher HM, Solaini L, et al. Gallbladder cancer. Am J Surg 2008;196:252–64.
[5] Stinton LM, Shaffer EA. Epidemiology of gallbladder disease: cholelithiasis and cancer. Gut Liver 2012;6:172–87.
[6] Hennedige TP, Neo WT, Venkatesh SK. Imaging of malignancies of the biliary tract: an update. Cancer Imaging 2014;14:14–35.
[7] Lee SE, Jang JY, Lim CS, et al. Systematic review on the surgical treatment for T1 gallbladder cancer. World J Gastroenterol 2011;17:174–80.
[8] Lau CSM, Zywot A, Mahendraraj K, et al. Gallbladder carcinoma in the United States: a population based clinical outcomes study involving 22,343 patients from the surveillance, epidemiology, and end result database (1973-2013). HPB Surg 2017;2017:1532835. doi: 10.1155/2017/1532835.
[9] Jang JY, Kim SW, Lee SE, et al. Differential diagnostic and staging accuracies of high resolution ultrasonography, endoscopic ultrasonography, and multidetector computed tomography for gallbladder polypoid lesions and gallbladder cancer. Ann Surg 2009;250:943–9.
[10] Zins M, Boulay-Coletta I, Molinie V, et al. Imaging of a thickened-wall gallbladder. J Radiol 2006;87(4 Pt 2):479–93.
[11] Zemour J, Marty M, Lapuyade B, et al. Gallbladder tumor and pseudotumor: diagnosis and management. J Visc Surg 2014;151:289–300.
[12] Pandey M, Sood BP, Shukla RC, et al. Carcinoma of the gallbladder: role of sonography in diagnosis and staging. J Clin Ultrasound 2000;28:227–32.
[13] Jindal G, Singal S, Nagi B, et al. Role of multidetector computed tomography (MDCT) in evaluation of gallbladder malignancy and its pathological correlation in an Indian rural center. Maedica (Buchar) 2018;13:55–60.
[14] Furlan A, Ferris JV, Hosseinzadeh K, et al. Gallbladder carcinoma update: multimodality imaging evaluation, staging, and treatment options. Am J Roentgenol 2008;191:1440–7.
[15] Hundal R, Shaffer EA. Gallbladder cancer: epidemiology and outcome. Clin Epidemiol 2014;6:99–109.
[16] Ito H, Matros E, Brooks DC, et al. Treatment outcomes associated with surgery for gallbladder cancer: a 20-year experience. J Gastrointest Surg 2004;8:183–90.
[17] Roa JC, Tapia O, Cakir A, et al. Squamous cell and adenosquamous carcinomas of the gallbladder: clinicopathological analysis of 34 cases identified in 606 carcinomas. Mod Pathol 2011;24:1069–78.
[18] Baig M, Guarino M, Petrelli N. Report on demographics of gall bladder cancer in Delaware and retrospective review of treatment strategies for gallbladder cancer in a large community cancer center. Surg Oncol 2016;25:86–91.
[19] Lee SW, Kim HJ, Park JH, et al. Clinical usefulness of 18F-FDG PET-CT for patients with gallbladder cancer and cholangiocarcinoma. J Gastroenterol 2010;45:560–6.
[20] Aloia TA, Jarufe N, Javle M, et al. Gallbladder cancer: expert consensus statement. HPB (Oxford) 2015;17:681–90.